IOP Conf. Series: Materials Science and Engineering **218** (2017) 012013 doi:10.1088/1757-899X/218/1/012013

The use of Spark Plasma Sintering method for high-rate diffusion welding of high-strength UFG titanium alloys

A V Nokhrin[1], V N Chuvil'deev[1], M S Boldin[1], A V Piskunov[1], N A Kozlova[1], M K Chegurov[1], A A Popov[1], E A Lantcev[1], V I Kopylov[1] and N Yu Tabachkova[2]

[1] Lobachevsky State University of Nizhny Novgorod, 23 Gagarin Ave., Nizhny Novgorod, 603950, Russia.
[2] The National University of Science and Technology MISiS, 4 Leninsky Ave., Moscow, 119991, Russia

E-mail: nokhrin@nifti.unn.ru

Abstract. The article provides an example of applying the technology of spark plasma sintering (SPS) to ensure high-rate diffusion welding of high-strength ultra-fine-grained UFG titanium alloys. Weld seams produced from Ti-5Al-2V UFG titanium alloy and obtained through SPS are characterized by high density, hardness and corrosion resistance.

1. Introduction

Today ultrafine-grained (UFG) metals and alloys obtained through Equal Channel Angular Pressing (ECAP) [1] generate particular interest among researchers. This is because UFG materials are found to have a unique combination of high strength and ductility [2-4], corrosion resistance [5] and radiation resistance [6], high-rate superplasticity [2, 7-9], etc.

One of the key challenges that currently prevent industrial introduction of UFG materials is the welding issue: traditional technologies such as argon arc welding or electron beam welding accompanied by metal meltdown fail to preserve the UFG structure with high physicochemical properties and performance characteristics in a weld seam. Solid phase technologies, such as classical diffusion welding or superplastic forming, require high temperatures and prolonged hold time which result in recrystallization processes and subsequent loss of any unique properties found with UFG materials.

The technology of Spark Plasma Sintering (SPS) offers great opportunities to obtain high-strength weld seams. SPS is based on the idea of high-rate heating (up to 2500^{o}C/min) of materials (powders, bulk materials, composites) in vacuum or inert atmosphere by means of passing millisecond high-power pulses (up to 5000 A) of direct pulse current through samples and simultaneous pressure application [10]. Such a combination enables high-density structures in metals, alloys and ceramics [11-13]. Advantages of SPS technology include an opportunity to reduce optimal sintering temperature for UFG materials [11-14]. High heating rates and an opportunity to ensure significant diffusion acceleration at reduced heating temperatures are essential to limit the process of grain growth and preservation of the original UFG structure in materials.

It shall be noted that ensuring a high-density weld seam with strength properties similar to those of the core material is a scientific challenge: a high-density structure presupposes prolonged hold time of the material at elevated temperatures, while a UFG structure may be preserved only if grain growth is

limited by means of reducing the heating temperature. This problem may be fixed if the conditions for high-rate heating of UFG materials are extended to include additional mechanisms of diffusion mass transfer related to nonequilibrium grain boundaries.

The goal of the paper is to study the SPS potential for diffusion welding of high-strength corrosion-resistant UFG titanium alloys used in nuclear engineering.

2. Materials. Experimental techniques

Samples of UFG titanium pseudo-α alloy Ti-4.73Al-1.88V (Russian industrial alloy PT3V) served as the materials of research. The UFG structure in materials under study was formed through Equal Channel Angular Pressing (ECAP). The number of ECAP cycles ranged from 1 to 4, while ECAP temperature varied from 450°C to 475°C. The rate of deformation during ECAP was 0.2-0.4 mm/s.
Diffusion welding was performed using a Dr.Sinter model SPS-625. Samples sized 7x7x3.5 mm obtained through spark cutting from UFG metal pieces sized 14×14×100 mm were welded. The level of surface roughness varied as a result of polishing with a diamond paste of various dispersion level (20-28 μm, 10-14 μm, 3-5 μm).

Diffusion welding was performed at the heating rate varying from 10 to 350°C/min, at the welding temperature ranging from 600 to 1140°C and under the pressure applied within the interval from 50 to 100 MPa. Diffusion welding time (at the temperature selected) varied from 0 to 90 minutes. The value and rate of shrinkage were controlled with a dilatometer being a part of a Dr.Sinter model SPS-625. The temperature was measured with a pyrometer Chino IR-AH focused on the side surface of samples. Structure studies were carried out using Jeol JSM-6490 scanning electron microscope and Jeol JEM-2100 transmission electron microscope. Pore size in weld seams was determined with Leica DM IRM metallographic microscope and Jeol JSM-6490 scanning electron microscope.

Microhardness was measured using Duramin Struers-5 microhardness tester with a 2 kg load. Electrochemical studies of samples were carried out in aqueous solution 10%HNO_3+0.2%HF using R-8 potentiostat-galvanostat (Russia) at room temperature. Analysis of Tafel areas of anodic potentiodynamic dependences 'potential – current density' in semi-logarithmic coordinates helped to determine corrosion current density (i_{cor}) which is proportionate to material corrosion rate in the given environment.

3. Experimental results

In the initial state the alloy is characterized by heterogeneous size distribution of grains. The average grain size varies from 10-20 μm to 50-100 μm (Fig. 1a). The average grain size after N=4 ECAP cycles is 0.2-0.5 μm (Fig. 1b).

Energy dispersive analysis reveals two types of grain boundaries (GB) in the structure of a coarse-grained alloy. Type one includes grain boundaries that we have termed 'clean'. These grain boundaries form an absolute majority. Average local concentration of aluminum in such GB is 3.8±0.9 wt.%, while average vanadium concentration is 1.9±0.2 wt.%. These figures differ little from concentrations of these elements in the material volume: average aluminum concentration in GBs is 3.6±0.9 wt.%, while vanadium concentration approximates ~1.4±0.2 wt.%.

The second GB type includes grain boundaries the local concentration of vanadium in which may reach 10 wt.% (Fig.2a). There are also single boundaries the local concentration of vanadium in which reaches 16-18 wt.%, while aluminum concentration is under 1 wt.%. The average value of aluminum concentration in the crystal lattice near such boundaries approximates ~4 wt.%, while vanadium concentration is ~1.6 wt.%.

It shall be emphasized that vanadium-rich GB are found in the areas of the titanium alloy structure where the average grain size substantially exceeds the average size of a fine-grained matrix (Fig. 1a).
Grain boundaries in UFG alloys are clean with no excess vanadium concentrations detected (Fig. 2b). Average vanadium concentration on UFG alloy grain boundaries is 1.9±0.3 wt.%, which is close to vanadium concentration in a crystal lattice 1.5±0.3 wt.%.

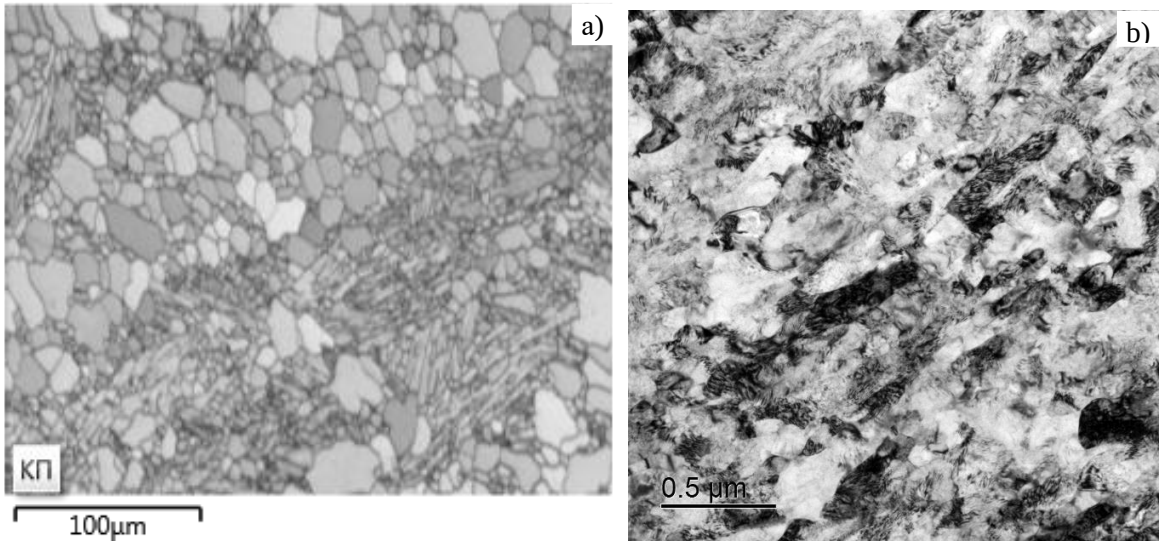

Figure 1. Titanium alloy structure in the original state (a) and after ECAP (b).

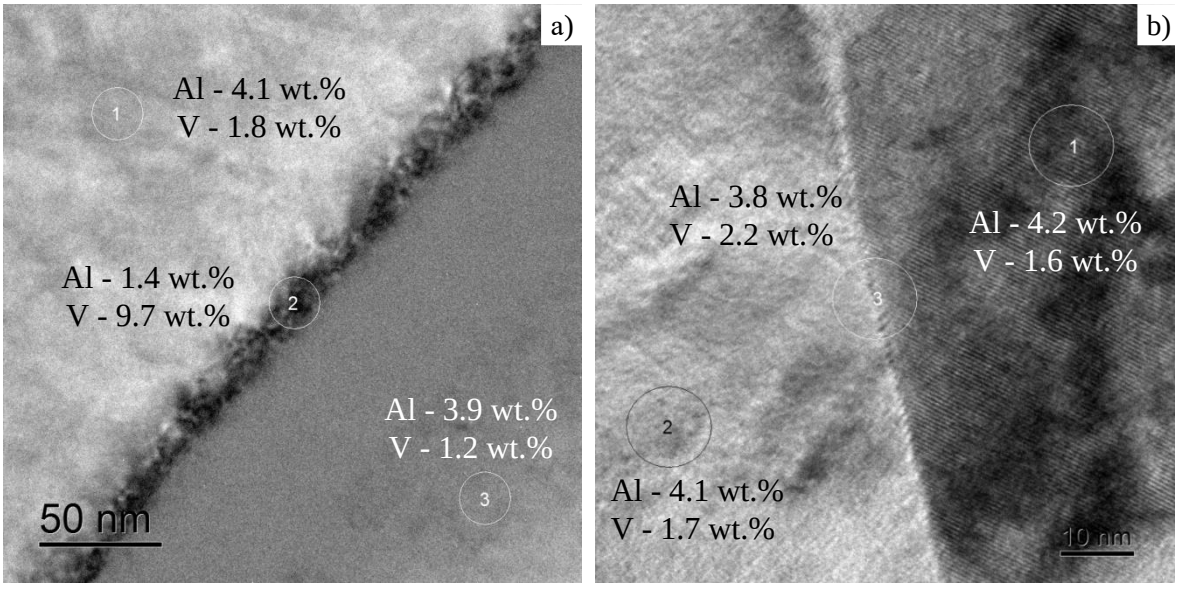

Figure 2. Results of energy dispersive analysis of grain boundaries in a coarse-grained alloy (a) and UFG titanium alloy (b).

Analysis of dependences of the shrinkage value (L) and the shrinkage rate (S) on the heating time prove that the welding process in UFG samples is more intensive: the shrinkage value and shrinkage rate in UFG titanium alloys appear to be much higher than similar characteristics in coarse-grained samples. The shrinkage value in coarse-grained alloys may be smaller than the thermal expansion contribution of the plant and remain unregistered by a dilatometer.

When summarized, the findings prove that under identical temperature and heating rate welding conditions, the average size and volume ratio of pores in UFG samples appear to be much smaller than in coarse-grained materials (Fig. 3).

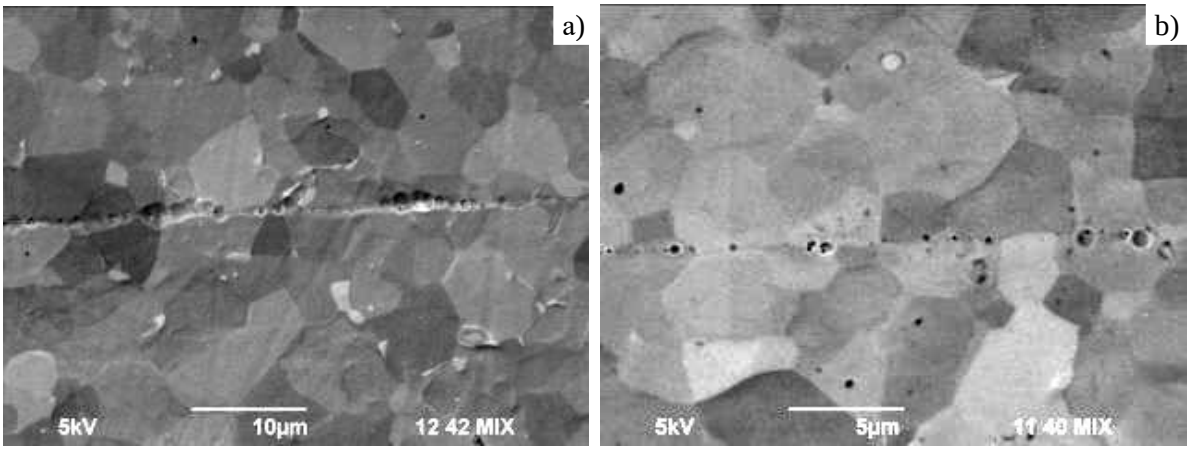

Figure 3. Weld seam produced from coarse-grained alloys (a) and UFG titanium alloys (b) obtained under identical temperature and heating rate welding conditions. Welding temperature 1030°C (above recrystallization temperature). Heating rate V=50°C/min, pressure 50 MPa.

The studies conducted show that the rate of weldability (shrinkage rate) in UFG alloys tends to increase if the heating rate grows. With coarse-grained alloys we observe an opposite effect: an increase in the heating rate leads to a decrease in the shrinkage rate (intensity of the welding process) (Fig. 4). We reckon that this effect arises from the following: high-rate heating (caused by overall reduction in the process time) brings down the intensity of grain boundaries migration and enables a more fine-grained structure (as compared to slower heating). This in turn decreases the typical scale of diffusion mass transfer *x*, the value of which in case of grain boundary diffusion is proportionate to grain size.

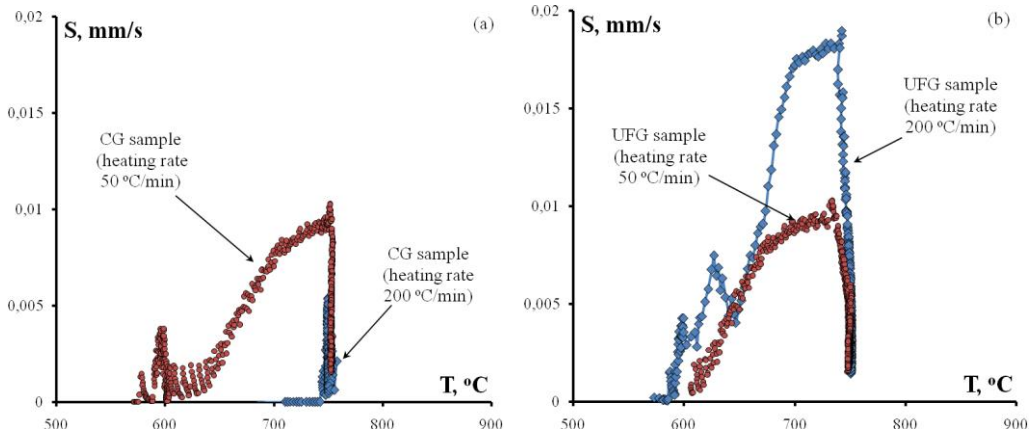

Figure 4. Comparison of temperature dependences on shrinkage rates for coarse-grained (CG) alloy samples (a) and UFG titanium alloy samples (b) with initial roughness level of 3-5 µm welded at heating rates of 50°C/min and 200°C/min under 80 MPa.

The research conducted into mechanical properties proves that the hardness of weld seams obtained though SPS (Fig. 5a) at temperatures below the temperature at the start of recrystallization process corresponds to the hardness of the core material measured at a distance of no less than the thickness of three walls of a welded item from the seam edge (Fig. 5b).

For the purposes of comparison, Fig. 5 (c, d) contains photos showing weld seams in UFG alloy samples obtained through argon arc welding (Fig. 5c) and electron beam welding (Fig. 5d).

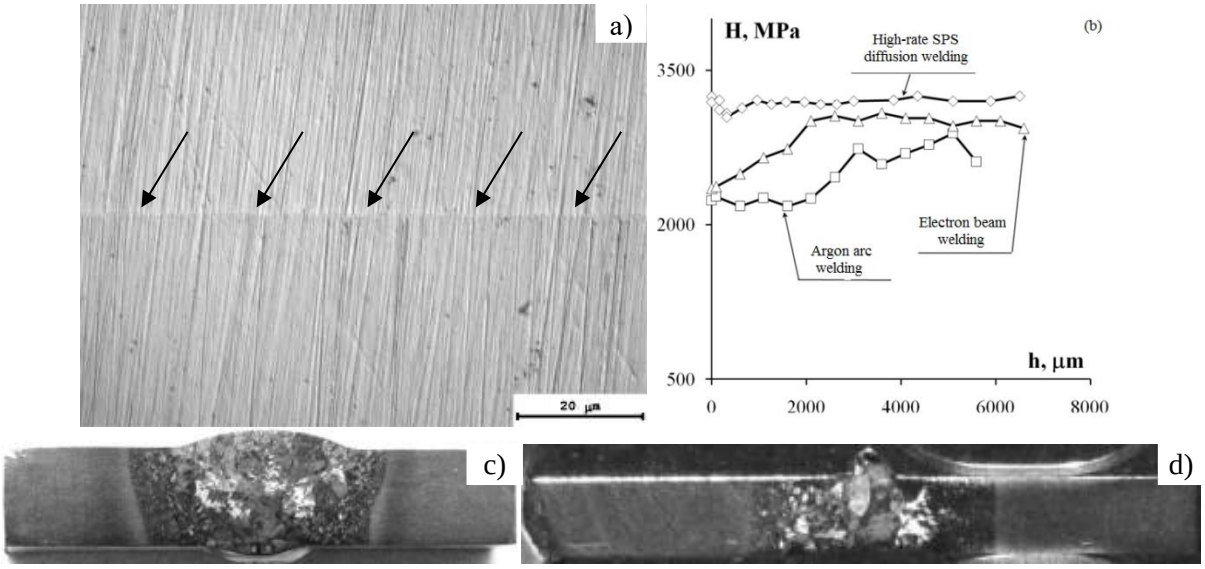

Figure 5. Microsection of a weld seam obtained though SPS (a), argon arc welding (c) and electron beam welding (d) of UFG alloy samples, microhardness distribution (b) in a cross section of UFG alloy weld seams obtained through a variety of welding technologies (h – distance from the seam center).

Table 1. Results of electrochemical studies of weld seams produced from coarse-grained and UFG titanium alloy (heating rate 10°C/min, pressure 50 MPa).

State	SPS welding temperature (°C)	Maximal current density (mA/cm^2)
Initial state (Coarse-grained)	600	1.15
	700	1.70
	800	0.25
UFG state (ECAP, N=4)	600	0.70
	700	1.00
	800	0.12

When comparing anodic potentiodynamic dependences for CG and UFG alloy samples after diffusion welding it should be noted that corrosion current density of weld seams from UFG titanium alloy within the temperature range of 600ºC to 800ºC appears to be less than current density of CG alloy weld seams ensured through similar welding modes.

With an increase in diffusion welding temperature, the difference in corrosion resistance between weld seams from CG and UFG titanium alloys grows: after diffusion welding at the temperature of 600ºC, the ratio of corrosion current density in weld seams produced from CG and UFG alloys was ~1.6, however when the welding temperature rose to 700ºC and 800ºC this ratio increased to 1.7 and ~2.1 respectively.

In our opinion, this effect is associated with recrystallization processes which underlie formation of a more homogeneous equiaxed structure in UFG titanium alloys, as well as with reduced local concentration of corrosive additives (V, Al) on UFG titanium alloy grain boundaries (see Fig. 2).

Analysis of anodic potentiodynamic dependences for UFG alloy weld seams obtained at different heating rates shows that irrespective of the original roughness, corrosion current density in samples obtained at a high heating rate (200°C/min) appears to be ~1.5 times less than in samples obtained at the heating rate of 50°C. Thus, corrosion current density i_{cor} for UFG alloy weld seams (with initial roughness of 3-5 μm) obtained at the heating rate of 50°C/min is 0.98 mA/cm^2, and at the heating rate of 200°C/min it equals 0.5 mA/cm^2. Current density for CG alloy weld seams obtained under similar conditions appears to be higher: for weld seams obtained at the heating rate of 50°C/min, the i_{cor} ~2.5 mA/cm^2, while those obtained at the heating rate of 200°C/min, the i_{cor} ~2.8 mA/cm^2.

Thus, the corrosion resistance of weld seams in UFG metal samples appears to be higher than the corrosion resistance of weld seams in CG materials.

4. Conclusion

SPS is proven to be an effective technology for high-rate diffusion welding of UFG titanium alloys. Optimization of temperature and rate conditions for SPS allows to produce UFG titanium alloy weld seams the hardness of which corresponds to that of the core material, whereas corrosion resistance is superior to that of the coarse-grained alloy weld seams.

Porosity of weld seams from UFG titanium alloys is found to be less than porosity of weld seams from coarse-grained titanium alloys obtained under similar conditions. An increase in the heating rate leads to higher intensity of diffusion welding with UFG titanium alloy samples, however with coarse-grained alloys higher heating rates result in reduced intensity of diffusion welding.

This effect is associated with the formation of UFG structure in a weld seam during high-rate diffusion welding, which helps to reduce the typical scale of diffusion mass transfer and typical time of diffusion 'exit' of pores from the weld seam due to the contribution of grain boundary diffusion the intensity of which significantly exceeds the diffusion intensity in a crystal lattice limiting the rate of diffusion welding of coarse-grained materials.

Acknowledgements

The authors are grateful for the support to the Russian Science Foundation (grant No. 16-13-00066).
The authors thank the Afrikantov Experimental Design Bureau for Mechanical Engineering (Nizhny Novgorod) for conducting argon arc welding and electron beam welding of UFG titanium alloys.

References

[1] Segal V M, Beyerlein I J, Tome C N, Chuvil'deev V N, Kopylov V I 2010 *Fundamentals and Engineering of Severe Plastic Deformation* (New York: Nova Science Publishers) 542 p.
[2] Valiev R Z, Langdon T G 2006 *Progress in Materials Science*. **51** (**7**) 881.
[3] Wang Y, Chen M, Zhou F, Ma E 2002 *Nature* **419 (6910**) 912.
[4] Chuvil'deev V N, Kopylov V I, Gryaznov M Yu, Sysoev A N, Ovsyannikov B V, Flyagin A A 2008 *Doklady Physics* **53 (11)** 584.
[5] Chuvil'deev V N, Kopylov V I, Bakmet'ev A M, Sandler N G, Nokhrin A V, Tryaev P V, Lopatin Yu G, Kozlova N A, Piskunov A V, Melekhin N V 2012 *Doklady Physics* **57 (1)** 10.
[6] Andrievskii R A 2011 *Nanotechnologies in Russia* **6 (5-6)** 357.
[7] Chuvil'deev V N, Shavleva A V, Nokhrin A V, Pirozhnikova O Ed, Gryaznov M Yu, Lopatin Yu G, Sysoev A N, Melekhin N V, Sakharov N V, Kopylov V I, Myshlayev M M 2010 *Physics of the Solid State* **52 (5)** 1098.
[8] Chuvil'deev V N, Nieh T G, Gryaznov M Yu, Sysoev A N, Kopylov V I 2004 *Scripta Materialia* **50 (6)** 861.
[9] Perevezentsev V N, Chuvil'deev V N, Kopylov V I, Sysoev A N, Langdon T G 2002 *Annales de Chimie: Science des Materiaux* **27 (3)** 36.
[10] Tokita M 2013 *Spark Plasma Sintering (SPS) Method, Systems, and Applications (Chapter 11.2.3)*. In Handbook of Advanced Ceramics (Second Ed.). Ed. Shigeyuki Somiya, Academic Press. 1149.
[11] Orlova A I, Volgutov V Yu, Mikhailov D A, Bykov D M, Skuratov V A, Chuvil'deev V N, Nokhrin A V, Boldin M S, Sakharov N V 2014 *Journal of Nuclear Materials* **446** (**1-3**) 232.
[12] Chuvildeev V N, Panov D V, Boldin M S, Nokhrin A V, Blagoveshensky Yu V, Sakharov N V, Shotin S V, Kotkov D N 2015 *Acta Astronautica* **109** 172.
[13] Chuvil'deev V N, Boldin M S, Dyatlova Ya G, Rumyantsev V I, Ordan'yan S S 2015 *Inorganic Materials* **51** (**10**) 1047.
[14] Chuvil'deev V N, Nokhrin A V, Baranov G V, Moskvicheva A V, Boldin M S, Kotkov D N, Sakharov N V, Blagoveshensky Yu V, Shotin S V, Melekhin N V, Belov V Yu 2013 *Nanotechnologies in Russia* **8 (1-2)** 108.